


Mechanisms of helix induction by the closed loop

Yuuki Yanagida¹ | Kiyomi Yoshida² | Mio Ohtomo² | Kazuo Fujiwara^{1,2} | Masamichi Ikeguchi^{1,2} 

¹Department of Biosciences, Soka University, Tokyo, Japan

²Department of Bioinformatics, Soka University, Tokyo, Japan

Correspondence

Masamichi Ikeguchi, Department of Biosciences, Soka University, 1-236 Tangi-machi, Hachioji, Tokyo 192-8577, Japan.
Email: ikeguchi@soka.ac.jp

Present address

Mio Ohtomo, Graduate School of Science, Kobe University, Hyogo, Japan.

Funding information

Japan Science and Technology Agency Support for Pioneering Research Initiated by the Next Generation, Grant/Award Number: JPMJSP2143

Review Editor: Aitziber L. Cortajarena

Abstract

Although various factors affecting the α -helix stability have been known, they are limited to short-range interactions that occur within the helix and its flanking regions. For better understanding of protein folding coupled with disulfide bond formation, the effect of disulfide bonds on the α -helix stability must be clarified. Using a protein fragment in which two helical regions are linked by a disulfide bond, we investigated the influence of the number of residues within the loop closed by the disulfide bond on the helix stability. We modified the number of residues within the loop by inserting glycine residues in the nonhelical region of the protein fragment. Circular dichroism and nuclear magnetic resonance spectra showed that increasing the number of inserted glycine residues led to a decreased helix content, while the helical regions remained unchanged. The helical fractions of individual residues were derived from chemical shift values, and their dependences on the number of inserted glycine residues were investigated. The results of this study and previous studies support the hypothesis that the helices are nucleated in the loop and propagated to both N- and C-termini. In addition, the fact that the helical fractions decrease with the number of inserted glycine residues suggests the mechanism in which the loop reduces the number of possible conformations, thereby promoting helix nucleation within the loop.

KEYWORDS

chemical shift, disulfide bond, helix-coil transition, protein folding

1 | INTRODUCTION

The α -helix is the most common secondary structure found in proteins. It is a helical structure consisting of 3.6 residues per turn, and the main chain amide group of one residue is hydrogen bonded to the carbonyl group of four residues ahead. It was first described in 1951 by Pauling et al. (1951), and its presence in the protein structure was evidenced when the crystal structure of myoglobin was determined by Kendrew et al. (1960). The helix-coil transition was observed for synthetic polypeptides (Doty et al., 1954), and the helix formation was formulated by the Zimm–Bragg theory

(Zimm & Bragg, 1959) or the Lifson–Roig theory (Lifson & Roig, 1961). Both theories define two parameters: nucleation and propagation parameters. For nucleation, three consecutive residues must take a helical φ – ψ angle to form the first hydrogen bond between the i th and $i + 4$ th residues. Therefore, the nucleation of the helix is generally difficult. Only one residue is needed to form an additional hydrogen bond for propagation, and once nucleation has taken place, subsequent propagation is relatively easy. The nucleation and propagation parameters for individual amino acids have been evaluated with tremendous effort (Chakrabarty & Baldwin, 1995; Scheraga et al., 2002).

This is an open access article under the terms of the [Creative Commons Attribution-NonCommercial-NoDerivs](https://creativecommons.org/licenses/by-nc-nd/4.0/) License, which permits use and distribution in any medium, provided the original work is properly cited, the use is non-commercial and no modifications or adaptations are made.

© 2025 The Author(s). *Protein Science* published by Wiley Periodicals LLC on behalf of The Protein Society.

Furthermore, statistical and experimental studies have revealed various factors that stabilized helices, such as capping interactions (Doig & Baldwin, 1995; Presta & Rose, 1988; Richardson & Richardson, 1988), charge-helix dipole interactions (Hol, 1985; Shoemaker et al., 1987; Wada, 1976), and side-chain interactions (Chakrabarty & Baldwin, 1995; Stapley et al., 1995). These helix-stabilizing factors known so far are the short-range interactions that occur within the helix and its flanking regions. In proteins, helices may interact with each other or with other secondary structural units, such as a β -sheet. In the case of disulfide-containing proteins, the helices may connect by disulfide bonds. Such long-range interactions frequently create a specific tertiary structure, and the contribution of individual interactions is difficult to analyze owing to the cooperativity of the tertiary structure. However, the effect of long-range interactions on helix stability can be analyzed in the folding intermediate or the partially unfolded state. Proteins, except for small proteins with less than 100 residues, assume a partially folded state during the early folding stages (Arai & Kuwajima, 2000; Chamberlain & Marqusee, 2000). Similar partially folded/unfolded states are observed under mild unfolding conditions such as at acidic or alkaline pH, at high temperature, and transiently under physiological conditions. These states are called “molten globule states” and have common characteristics. They have secondary structures that are similar to but not identical to the native secondary structure, their molecular sizes are compact like the native structures, they lose the side-chain packing, and they show diffuse unfolding transition (Ptitsyn, 1995). In this study, we address how the loop formed by a disulfide bond affects the stability of the helix. Although many studies report that the disulfide bond stabilizes or destabilizes the secondary structure in the folding intermediates (Horng et al., 2003; Ikeguchi et al., 1992; Ikeguchi & Sugai, 1989; Moriarty et al., 2000; Peng et al., 1995; Yamada et al., 2006), the effect of the disulfide bond on the specific secondary structural unit has not been investigated.

Previous studies have shown that equine β -lactoglobulin (ELG) forms a molten globule state at acidic pH (Ikeguchi et al., 1997). ELG is a 162-residue globular protein with eight antiparallel β -strands (labeled A–H) and a C-terminal helix downstream of the H-strand. In the molten globule state (A state), the region corresponding to the H-strand and C-terminal helix assumes a non-native helix in addition to a β -hairpin of F and G strands (Nakagawa et al., 2006). At lower temperatures, the molten globule is transformed to the cold-denatured state (C state), which has an expanded conformation, and the FG-hairpin is converted to the helix (Nakagawa et al., 2006, 2007; Yamada et al., 2005). The secondary structures in the C state can be mimicked in a fragment of ELG (residue: 88–142), which was named CHIBL (the core

of the helical intermediate of β -lactoglobulin) (Nakagawa et al., 2007). Yamamoto et al. (2011) analyzed the detailed structure of the F strand-truncated CHIBL (CHIBL Δ F) using nuclear magnetic resonance (NMR) and revealed that α -helices are formed around residues 98–107 (corresponding to G-strand region of the full length protein) and 114–135 (corresponding to H-strand and C-terminal helix regions of the full length protein). In this paper, we call these two helices the N-terminal helix and the C-terminal helix, respectively. These two helices are linked by the disulfide bond between Cys106 and Cys119 (Figure 1). Note that the structure is not persistent. At ambient temperatures, the structure of CHIBL Δ F is considered to be the ensemble of various conformations, including a conformation in which only the N-terminal helix is formed, a conformation in which only the C-terminal helix is formed, and a conformation in which both helices are formed. Furthermore, the lengths of the helices would be various. Circular dichroism (CD) spectra show that the α -helical content of CHIBL Δ F is reduced when the disulfide bond is cleaved. Short peptide fragments (97–110 and 111–138) do not form stable helices, and the sum of the spectra of these two peptides is similar to that of reduced CHIBL Δ F (Yamamoto et al., 2011). These results show that α -helices in CHIBL Δ F are stabilized by the disulfide bond. The authors suggested that the helices are stabilized because the helix nucleation is enhanced when the closed loop is formed by disulfide bond formation (Yamamoto et al., 2011). The aim of the present study was to verify this hypothesis.

2 | RESULTS

2.1 | Absence of tertiary interactions in CHIBL Δ F

A possible mechanism by which the disulfide bond stabilizes the α -helices is that the disulfide bond increases the effective concentration of interacting side chains for stabilization of α -helices. If residues neighboring Cys106 and Cys119 interact with each other so that α -helices are stabilized, the interresidue nuclear Overhauser effects (NOEs) may be observed between such pairs of interacting residues. Although we previously investigated 15 N-edited NOESY spectra of CHIBL Δ F, we could find no long-range NOEs (Yamamoto et al., 2011). Therefore, the two helical regions do not pack together tightly. To further confirm the absence of interactions between residues in the two helical regions, we synthesized peptide GssH in which the peptide 97–110 (hereafter called the G-peptide) and H-peptide (corresponding to residue 111–128) were linked by the disulfide bond between Cys106 and Cys119. Figure 2 shows the CD spectrum of GssH compared with the spectra of G-peptide and H-peptide

FIGURE 1 Schematic diagram of the sequence and structural model of CHIBLΔF. The ribbon model was created by MODELER (Sali & Blundell, 1993). The numbers displayed in the diagram represent the parent protein residue numbers.

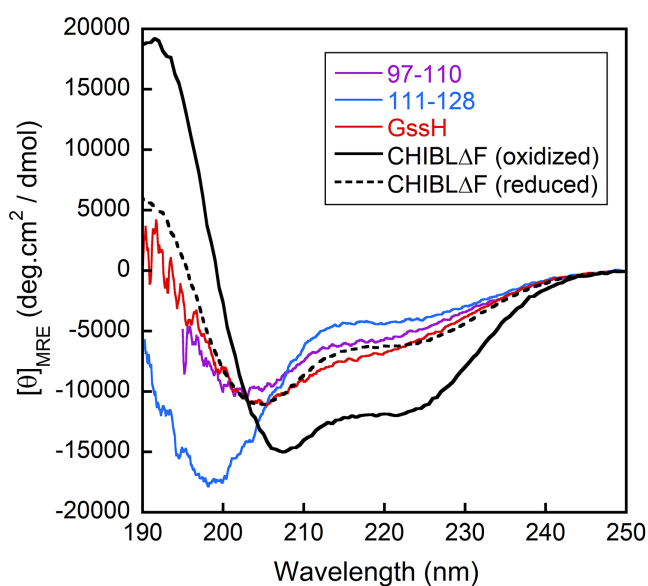
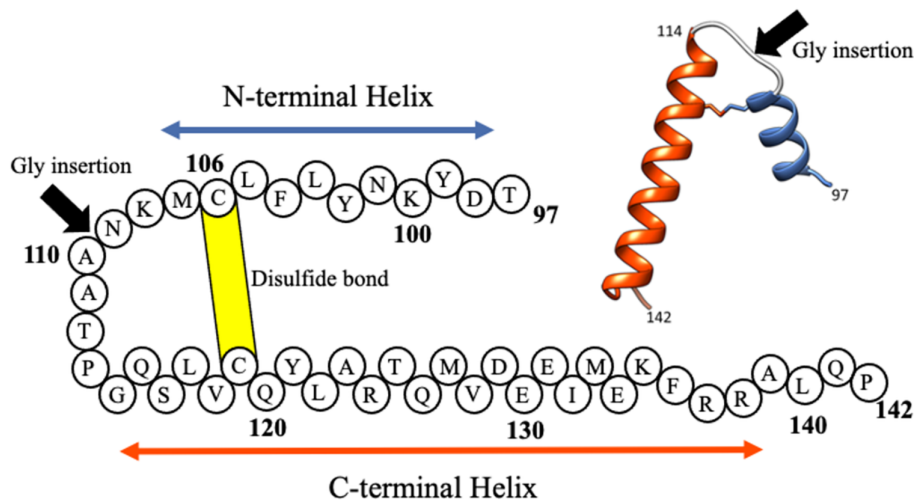


FIGURE 2 CD spectra of G-peptide (97–110), H-peptide (111–128), and GssH, oxidized CHIBLΔF, and reduced CHIBLΔF in 0.1 M phosphoric acid (pH 1.6) at 25°C.

alone. The spectrum shows that the helical content of GssH is comparable with that of disulfide-reduced CHIBLΔF. Therefore, the helix promotion by the disulfide bond is not caused by the increased effective concentration of interacting side chains.

2.2 | Closed loop effect on helix stabilization

As an alternative mechanism of helix stabilization by the disulfide bond, Yamamoto et al. (2011) proposed the mechanism in which the helix nucleation is enhanced in the closed loop because of the restricted conformational freedom. If their assumption is correct, we can expect that the population of α -helices would be

reduced if the loop were elongated by inserting several glycine residues in the middle. To confirm this, we made CHIBLΔF variants in which one, three, and seven glycine residue(s) were inserted into the loop region, and their helical fraction was compared with CHIBLΔF. Hereafter, CHIBLΔF is called G0, and one-, three-, and seven-glycine-inserted variants are called G1, G3, and G7, respectively.

The CD spectra of G0, G1, G3, and G7 in 0.1 M phosphoric acid are shown in Figure 3a, indicating that all protein fragments have α -helical structures. As the number of inserted glycine residues increased, the mean residue ellipticity ($[\theta]_{\text{MRE}}$) at 222 nm increased, indicating that elongating the loop destabilizes the helix. The temperature dependence of the $[\theta]_{\text{MRE}}$ at 222 nm is shown in Figure 3b. For all fragments, the $[\theta]_{\text{MRE}}$ at 222 nm gradually increased with temperature. It is known for the molten globule states (Griko & Privalov, 1994; Ikeguchi & Sugai, 1989; Yamada et al., 2005; Yutani et al., 1992) and short peptides (Richardson & Makhatadze, 2004; Scholtz et al., 1991) that thermal helix-coil transitions are too broad to observe the entire transition within the experimentally accessible temperature range. Therefore, the temperature dependence of $[\theta]_{\text{MRE}}$ shown in Figure 3b is interpreted as a part of a broad thermal unfolding transition. Because the nearly identical $[\theta]_{\text{MRE}}$ values of the fully helical state and of the unfolded state are expected for G0–G7, Figure 3b shows that the glycine insertion (Gly-insertion) destabilizes the helix. However, it is unclear whether it destabilizes only the N-terminal helix or only the C-terminal helix or both helices. To clarify this, we measured the chemical shifts of individual residues using heteronuclear multidimensional NMR spectroscopy.

The ^1H – ^{15}N HSQC spectra of G1, G3, and G7 at 12°C are shown in Figure 4 and Supplementary Figure S1. The peak assignment is presented as the residue number in the whole polypeptide of ELG.

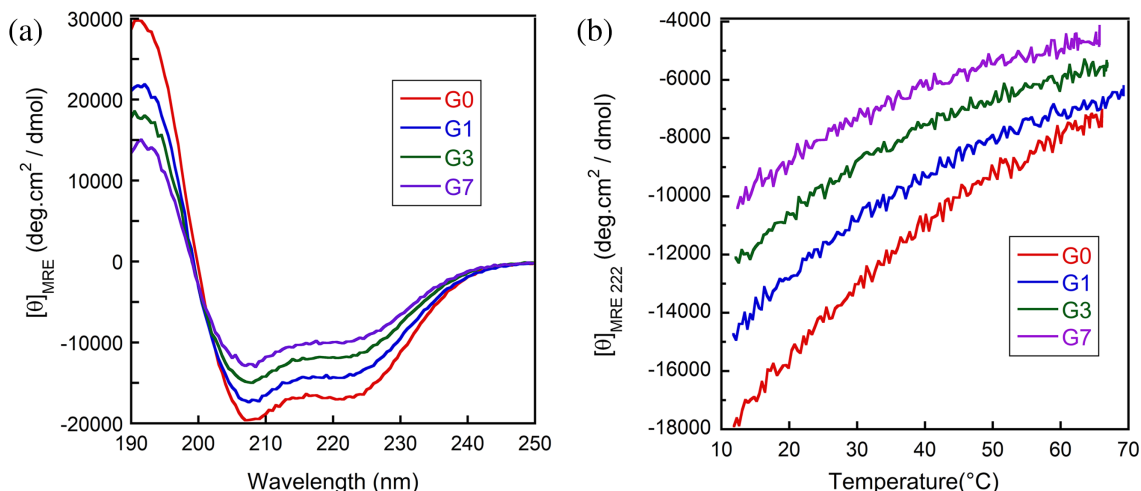


FIGURE 3 (a) CD spectra of G0, G1, G3, G7 at 0.1 M phosphoric acid, 12°C. (b) Thermal transition curves of G0, G1, G3 and G7 monitored by $[\theta]_{\text{MRE}}$ at 222 nm.

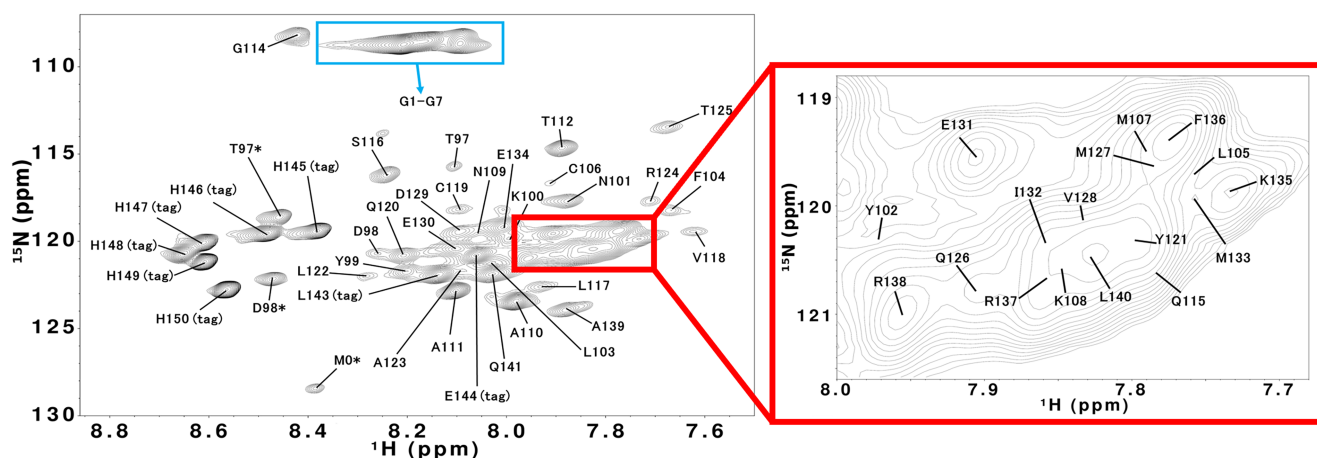


FIGURE 4 ^1H - ^{15}N HSQC spectrum of G7 in 0.1 M phosphoric acid (90% H_2O /10% D_2O) at 12°C. Assigned peaks are labeled. The sample contained formylated N-terminal methionine (labeled M0*) and free N-terminal methionine. Because of the heterogeneity, two cross-peaks labeled with asterisks are present for certain residues (T97, D98). Cross peaks for the hexa-histidine sequence used for purification are labeled as (tag).

Backbone ^1HN , $^1\text{H}\alpha$, ^{13}CO , ^{15}N , $^{13}\text{C}\alpha$, and $^{13}\text{C}\beta$ assignments were obtained for all residues (Table S1–S4 in the Supporting Information). Chemical shifts are derived from primary shifts (chemical shifts specific to individual amino acids) and secondary shifts (chemical shifts derived from the three-dimensional structure). The secondary shift is often used as an indicator of secondary structures. In general, when forming α -helices, the $^1\text{H}\alpha$ and $^{13}\text{C}\beta$ chemical shifts are shifted lower than the random coil values, while the $^{13}\text{C}\alpha$ and ^{13}CO chemical shifts are shifted higher than the random coil values. The shift is usually opposite to the aforementioned shifts when forming β -sheets. In this study, the chemical shifts of linear peptides of six residues (Wishart, Bigam, Holm, et al., 1995) were used for the first-order shifts, and the second-order shifts of $^1\text{H}\alpha$, $^{13}\text{C}\beta$, $^{13}\text{C}\alpha$, and ^{13}CO for G0–G7 were calculated and

are shown in Figure 5. The secondary shifts of $^{13}\text{C}\alpha$ and ^{13}CO showed low field shifts at residue numbers 98–107 and 114–135. A high field shift was observed in the same region for the secondary shift of $^1\text{H}\alpha$. This was similar for all helix regions of G0–G7, but the shift amount decreased as the number of inserted glycine residues increased. These results show that the helical regions are essentially the same for all G0–G7 and the helical population of each residue decreases with the elongation of the loop.

Unfolded proteins are heterogeneous in solution and cannot be described as a single structure. Therefore, they need to be characterized as a probability distribution. Camilloni et al. (2012) have developed a method called $\delta^2\text{D}$, which determines the populations of secondary structures (α -helix, β -strand, random coil, and polyproline II) for each residue. The helical

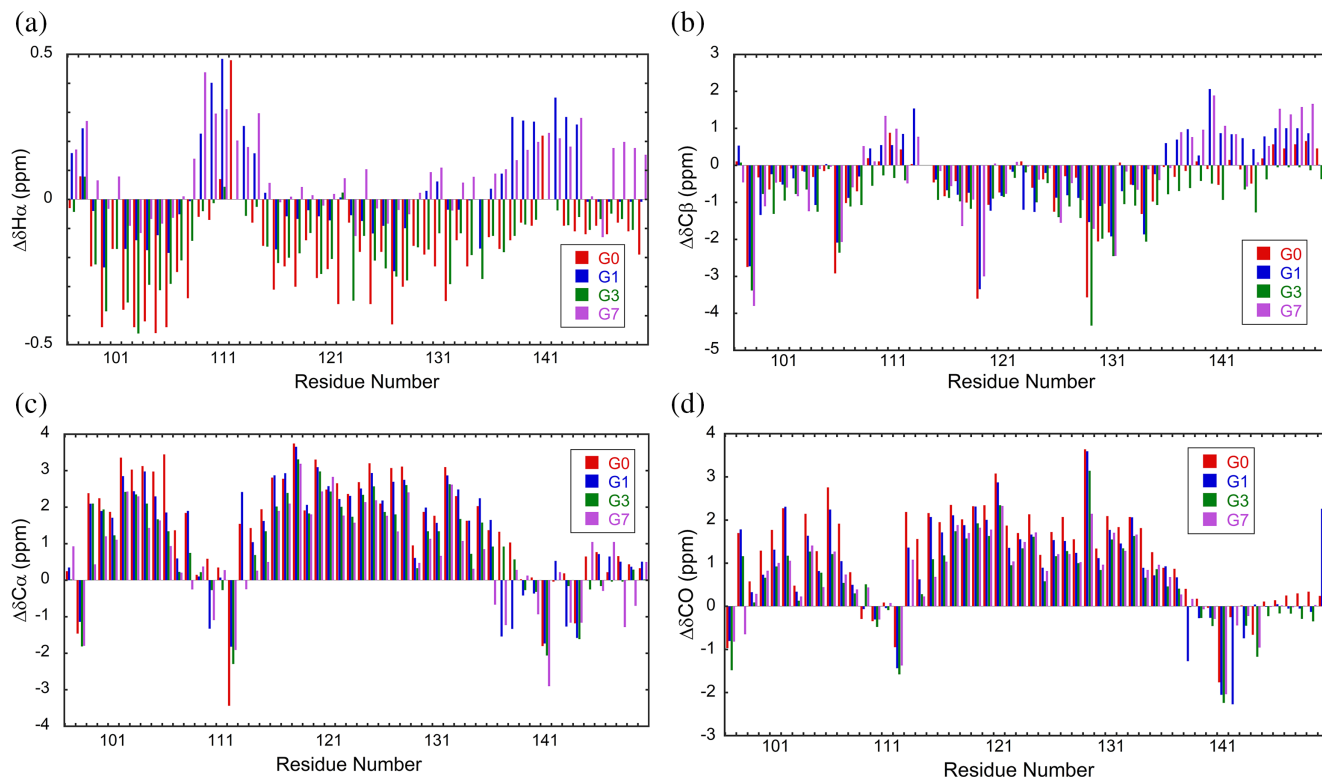


FIGURE 5 Chemical shift deviations of G0–G7 chemical shifts from random coil shift. (a) $^1\text{H}\alpha$, (b) $^{13}\text{C}\beta$, (c) $^{13}\text{C}\alpha$, (d) ^{13}CO .

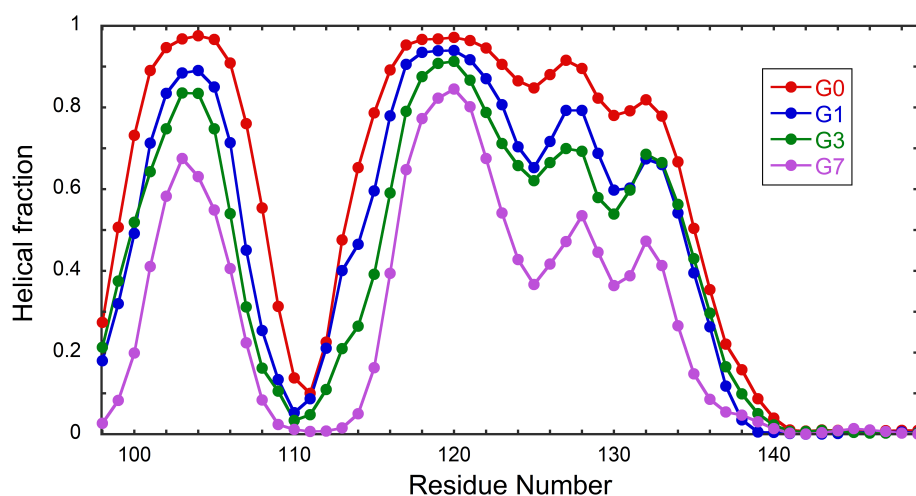


FIGURE 6 Helical fractions of individual residues of G0–G7 calculated from chemical shifts using a $\delta 2\text{D}$ program.

fractions of individual residues in G0–G7 were calculated using $\delta 2\text{D}$ from the $^1\text{H}\alpha$, $^{13}\text{C}\beta$, $^{13}\text{C}\alpha$, ^{13}CO , N, and HN chemical shifts (Figure 6). Figure 6 shows that the helical regions were essentially the same for all fragments and that the Gly-insertion reduced helical fractions in the entire region. The average helical fraction was 56%, 45%, 40%, and 25% for G0, G1, G3, and G7, respectively. A plot of CD values ($[\theta]_{\text{MRE}}$) at 222 nm against the average helical fractions shows a straight line (Supplementary Figure S2), indicating that

the helical fraction estimated by $\delta 2\text{D}$ is consistent with the CD result. The line indicates that $[\theta]_{\text{MRE}}$ at 0% helical fraction is $-3900\text{deg}\cdot\text{cm}^2\cdot\text{dmol}^{-1}$, which is consistent with $[\theta]_{\text{MRE}}$ of G7 at high temperatures (Figure 3b). $[\theta]_{\text{MRE}}$ at 100% helical fraction is $-26,200\text{deg}\cdot\text{cm}^2\cdot\text{dmol}^{-1}$. Although this value is larger than the value proposed for 100% helix (e.g., $-38,800\text{deg}\cdot\text{cm}^2\cdot\text{dmol}^{-1}$ at 12°C (Scholtz et al., 1991)), the value is reasonable because not all residues can assume the helical structure due to the

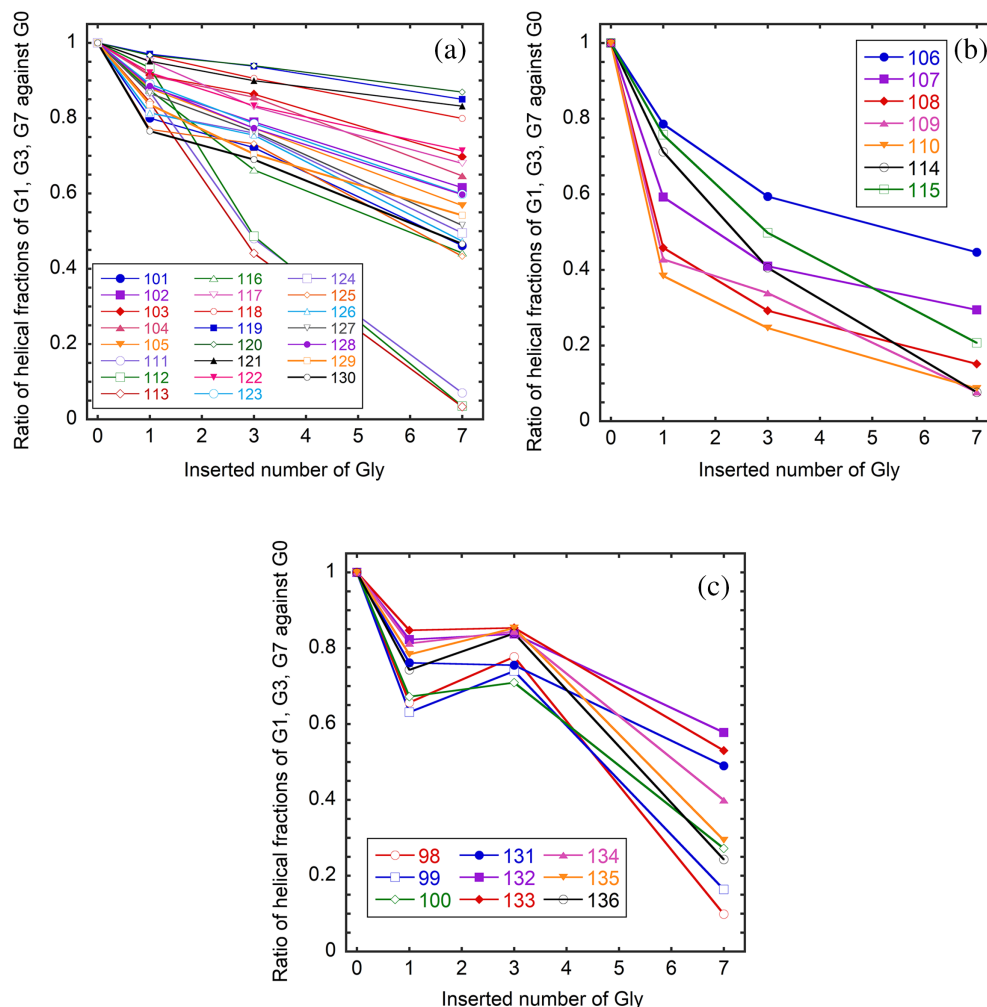


FIGURE 7 The dependences of the helical fractions of individual residues on the number of inserted glycine residues. The dependences are classified into group 1 (a), group 2 (b), and group 3 (c).

loop formation. Furthermore, the experimental result showed that the residues beyond 140 do not assume the helix, irrespective of the number of inserted glycine residues.

To investigate the effect of Gly-insertion on the helical fractions of individual residues, the ratios of helical fractions of G1, G3, and G7 against that of G0 were plotted against the number of inserted glycine residues (Figure 7). For clarity of Figure, we categorized the residues into three groups. Most residues (group 1) show a linear decrease in the helical fraction with the number of inserted glycine residues. Within this group, residues 111–113 are remarkable, and their helical fractions diminish in G7. The second group consists of the residues just ahead of the inserted position (106–110) and the residues 114 and 115, which show a significant decrease in the helical fractions when only one glycine residue is inserted. The third group consists of residues 98–100 and 132–136, that is, the residues located at the end of the helix far away from the Gly-inserted position. Their helical fractions do not significantly decrease in G1 and G3 but show an abrupt decrease in G7.

3 | DISCUSSION

The cross-links, such as disulfide bonds, stabilize the native state by destabilizing the unfolded state (Betz, 1993; Zhang et al., 1994). The stability of the native conformation is evaluated through the free energy difference between the native and unfolded states. When cross-links are introduced into the random coil polypeptide, which is an ideal model of the unfolded state, the number of possible conformations is reduced so that the entropy of the unfolded state is decreased (Lin et al., 1984; Poland & Scheraga, 1965). Therefore, the free energy level of the unfolded state increases. If the cross-link does not significantly affect the native conformation, the free energy level of the native state is unchanged (the enthalpy change for making a cross-link is not included in this consideration because it is the same for both the native and unfolded states). As a result, the free energy difference between the native and unfolded states increases, making the native state more stable. Is this mechanism of structural stabilization applicable to

flexible conformations such as CHIBL Δ F? The answer is clearly no. In contrast to the native protein conformations, the structure of CHIBL Δ F is so flexible that the number of possible conformations is reduced when a cross-link is introduced. Yamamoto et al. (2011) have proposed that the nucleation of α -helix is enhanced in the closed loop. The helix formation was formulated by the Zimm–Bragg theory (Zimm & Bragg, 1959) or the Lifson–Roig theory (Lifson & Roig, 1961). Both theories define two parameters: nucleation and propagation parameters. For nucleation, three consecutive residues must adopt a helical φ – ψ angle to form the first hydrogen bond between the i th and $i + 4$ th residues. Therefore, the nucleation of the helix is generally laborious. Only one residue must be fixed to form an additional hydrogen bond for propagation once nucleation occurs. This makes propagation easier than nucleation. Yamamoto et al. (2011) have suggested that the entropy cost of nucleation is smaller in the closed loop than in the open chain. To support their suggestion, we estimated the possibility to take a helical φ – ψ angle as follows. The probability of taking a certain φ – ψ angle is assumed to obey the Boltzmann distribution based on the intrinsic potential energy of a residue depending on the φ – ψ angle. As the potential energy, we used the single amino acid potential calculated for a formyl alanine amide in water using a quantum chemical calculation based on a self-consistent isodensity polarizable continuum model for solute–solvent interactions (Iwaoka et al., 2006). The potential energy was calculated for each 15° of φ and ψ angles. If the population of the lowest energy angles ($\varphi = -90^\circ$ and $\psi = -15^\circ$) is defined as unity, the summation of relative populations of all φ – ψ angles is 20.4 (Supplementary Figure S3). Of this number, 1.84 (9%) are compatible with α -helix (see Supplementary Figures S3 and S4). If the disulfide cross-link restricts the total number of conformations, how is the number of conformations defined by a certain φ – ψ angle changed? A theoretical study has shown that the number of independent variables reduces by six when forming a closed loop (Go & Scheraga, 1970; Wedemeyer & Scheraga, 1999). However, it is currently not known how reducing the degree of freedom corresponds to restricting the freedom of individual residues. We assumed that high-energy conformations are selectively excluded, leading to an increase in the probability of the helical φ and ψ angles because the energy of helical φ and ψ angles is relatively low. As a result, the helix nucleation in the loop closed by the disulfide cross-link (106–119) would be promoted. This nucleation promotion effect should be significant when the loop is small (the residue included in the loop is few). Therefore, the decrease in the helical fractions of the residues 106–119 with the increasing number of inserted glycine (Figure 6) is probably due to the reduced probability of the helix

nucleation. The low helix propensity of the inserted glycine may affect the helical fractions of neighboring residues. To minimize this effect, the Gly-insertion point was selected between positions 109 and 110, where G0 inherently shows low helical propensity (Figure 6). The low helical fraction in this region is probably due to the strong helix breaker proline at 113. The influence of Gly-insertion can be clearly observed in the dependence of the helical fractions of individual residues (Figure 7). The many residues within the loop closed by the disulfide bond 106–119 show responses classified in group 2. The residues close to the inserted position (108, 109, and 110) in group 2 show large responses to the Gly-insertion (Figure 7b). Although we classified residues 111, 112, and 113 into group 1, they show characteristic large responses to the Gly-insertion (Figure 7a). At least part of these responses may be due to the low helix propensity of glycine. Although residues 114 and 115 are far from the insertion position, they show responses comparable to 108–110. Rather than the distance in sequence from the insertion position, the distance from Cys106 or Cys119 seems to be related to the response against the number of inserted glycine residues.

Once the helix is nucleated in the loop, it propagates to the N- and C-terminus directions beyond residues 106 and 119, respectively. Therefore, the helical fractions of residues 98–105 and 120–139 also decrease with the inserted glycine numbers (Figures 6 and 7). The effect of glycine insertion disappears around residue 140 due to the existence of Pro142. In contrast, the effect continues to the N-terminus. The residues located at the end of the helix (group 3) show the largest responses when seven glycine residues are inserted (Figure 7c). The entropic effect on helix nucleation is expected to be greater when a larger number of residues are inserted than when only one glycine residue is inserted. The fact that the responses of the residues in group 3 are observed at the residues close to the N- and C-terminus of the protein fragment suggests that the helices are mainly nucleated in the loop closed by the disulfide bond and propagated to the N- and C-terminus.

4 | CONCLUSIONS

This study is the first to address the effect of cross-links on the conformational properties of individual residues in a flexible polypeptide. It was shown that the helices are destabilized with an increase in the number of residues within the loop formed by the disulfide bond. The results can be interpreted as follows. As the residue number forming the loop increases, the number of conformations within the loop increases. As a result, the entropy cost for assuming the helical φ and ψ angles

increases, so that the helix nucleation is suppressed. This interpretation is supported by the fact that the helical fractions of the residues outside of the loop are changed depending on the number of glycine residues inserted. These findings are important for understanding the disulfide folding of proteins (Wedemeyer et al., 2000).

5 | MATERIALS AND METHODS

5.1 | Construction of genes and expression vectors

The expression vectors for G1 and G3 were constructed using the QuikChange method, using a pET21a vector with the G0 gene inserted as a template with appropriate primers. The sequence was confirmed by Eurofins Genetics Ltd. The G7 gene was synthesized by Eurofins Genetics Ltd. and inserted into pET21a. *Escherichia coli* BL21 (DE3) competent cells were transformed with one of the expression vectors.

5.2 | Expression, refolding, and purification

To obtain nonisotopically labeled G0, G1, G3, and G7, *E. coli* cells harboring the corresponding expression vectors were cultured in a Luria–Bertani medium, and the protein expression was induced. All protein fragments were present in the insoluble fraction of the cell lysate and were solubilized in 50 mM Tris–HCl (pH 8.0) containing 6 M urea, 0.5 mM hydroxyethyl disulfide, and 5 mM β -mercaptoethanol. The latter two reagents were added for disulfide bond formation. The solubilized protein was applied to a Ni^{2+} -chelate column equilibrated with 50 mM Tris–HCl, pH 8.0, containing 10 mM imidazole, 0.5 M NaCl, and 6 M urea. It was then eluted using a linear gradient of 100–600 mM imidazole. The fractions containing the protein fragment were dialyzed against water, causing the protein fragment to precipitate in the dialyzing bag. Precipitates were collected through centrifugation, washed with distilled water, and then lyophilized. The purity was confirmed using sodium dodecyl sulfate–polyacrylamide gel electrophoresis and reversed-phase high-performance liquid chromatography (HPLC). The molecular weight was confirmed using an Autoflex II TOF/TOF mass spectrometer (Bruker Daltonics).

Uniformly $^{15}\text{N}/^{13}\text{C}$ -labeled samples were obtained by culturing *E. coli* that harbored the expression plasmid in an M9 medium, including $^{15}\text{NH}_4\text{Cl}$ and $^{13}\text{C}_6$ -glucose (Cambridge Isotope Laboratories) as the sole nitrogen and carbon source, respectively. The labeled protein fragments were purified as described above.

5.3 | Peptide synthesis

The peptide 97–110 (G-peptide) was synthesized and purified as described previously (Yamamoto et al., 2011). Peptide 111–128 (H-peptide) was synthesized, and its N- and C-termini were acetylated and amidated, respectively, as described previously. A disulfide-linked peptide GssH was prepared by forming a 106–119 disulfide bond in the mixture of purified G and H-peptides dissolved in 5 mM NH_4HCO_3 containing 40 μM CuCl_2 . The reaction proceeded overnight under an oxygen atmosphere. Using reverse-phase HPLC, GssH was separated from other products such as G-peptide dimer cross-linked (GssG), H-peptide dimer cross-linked (HssH), unreacted G-peptide, and unreacted H-peptides. The molecular weight was confirmed using an Autoflex II TOF/TOF mass spectrometer (Bruker Daltonics).

5.4 | CD spectroscopy

CD spectra were recorded with a 1-mm pathlength quartz cuvette using a Chirascan CD spectrometer (Applied photophysics). Peptide concentrations were determined spectroscopically using the molar absorption coefficient $\epsilon_{280} = 3840 \text{ M}^{-1} \text{ cm}^{-1}$ for G0, G1, G3, G7, and GssH, $\epsilon_{280} = 2560 \text{ M}^{-1} \text{ cm}^{-1}$ for G-peptide, and $\epsilon_{280} = 1280 \text{ M}^{-1} \text{ cm}^{-1}$ for H-peptide. The molar absorption coefficients were calculated from the number of Tyr residues and the molar extinction coefficient of Tyr, $1280 \text{ M}^{-1} \text{ cm}^{-1}$ (Gill & von Hippel, 1989).

5.5 | NMR spectroscopy

The lyophilized $^{15}\text{N}/^{13}\text{C}$ -labeled sample was dissolved in 0.1 M 90% $\text{H}_3\text{PO}_4/10\%$ D_3PO_4 , pH 1.6, to a protein concentration of approximately 1 mM. Sodium 3-trimethylsilyl-2,2,3,3- ^2H propionate served as the internal ^1H reference (0.003 ppm), and ^{13}C and ^{15}N chemical shifts were indirectly referenced (Wishart, Bigam, Yao, et al., 1995). Spectra were obtained using a Bruker AVANCE III HD spectrometer operating at 600 MHz and using a 5-mm TXI probe at 12°C . ^1H – ^{15}N HSQC, HNCO, HN(CA)CO, CBCA(CO)NH, HNCACB, HBHA(CO)NH, and HBHANH spectra were recorded for main chain assignments. NMR data were processed using NMRPipe (Delaglio et al., 1995), and resonance assignments were performed using MagRO-NMRView (Kobayashi et al., 2007, 2012).

AUTHOR CONTRIBUTIONS

Yuuki Yanagida: Investigation; writing – original draft; visualization; validation; funding acquisition. **Kiyomi Yoshida:** Investigation; writing – review and editing. **Mio Ohtomo:** Investigation; writing – review and

editing. **Kazuo Fujiwara:** Writing – review and editing; resources; formal analysis. **Masamichi Ikeguchi:** Writing – review and editing; supervision; resources; conceptualization; project administration.

ACKNOWLEDGMENTS

We would like to express our profound gratitude to Professor Michio Iwaoka of Tokai University for providing the energy values for the potential energy map.

FUNDING INFORMATION

This work was supported in part by Japan Science and Technology Agency Support for Pioneering Research Initiated by the Next Generation, Japan Grant Number JPMJSP2143 to YY.

DATA AVAILABILITY STATEMENT

The data that support the findings of this study are available from the corresponding author upon reasonable request.

ORCID

Masamichi Ikeguchi  <https://orcid.org/0000-0003-1190-1130>

REFERENCES

- Arai M, Kuwajima K. Role of the molten globule state in protein folding. *Adv Protein Chem.* 2000;53:209–82.
- Betz SF. Disulfide bonds and the stability of globular proteins. *Protein Sci.* 1993;2(10):1551–8.
- Camilloni C, de Simone A, Vranken WF, Vendruscolo M. Determination of secondary structure populations in disordered states of proteins using nuclear magnetic resonance chemical shifts. *Biochemistry.* 2012;51(11):2224–31.
- Chakrabarty A, Baldwin RL. Stability of α -helices. *Adv Protein Chem.* 1995;46:141–76.
- Chamberlain AK, Marqusee S. Comparison of equilibrium and kinetic approaches for determining protein folding mechanisms. *Adv Protein Chem.* 2000;53:283–328.
- Delaglio F, Grzesiek S, Vuister GW, Zhu G, Pfeifer J, Bax A. NMRPipe: a multidimensional spectral processing system based on UNIX pipes. *J Biomol NMR.* 1995;6(3):277–93.
- Doig AJ, Baldwin RL. N- and C-capping preferences for all 20 amino acids in alpha-helical peptides. *Protein Sci.* 1995;4(7):1325–36.
- Doty P, Holtzer AM, Bradbury JH, Blout ER. Polypeptides. II. The configuration of polymers of γ -benzyl-L-glutamate in Solution. *J Am Chem Soc.* 1954;76(17):4493–4.
- Gill SC, von Hippel PH. Calculation of protein extinction coefficients from amino acid sequence data. *Anal Biochem.* 1989;182(2):319–26.
- Go N, Scheraga HA. Ring closure and local conformational deformations of chain molecules. *Macromolecules.* 1970;3(2):178–87.
- Griko YV, Privalov PL. Thermodynamic puzzle of apomyoglobin unfolding. *J Mol Biol.* 1994;235(4):1318–25.
- Hol WGJ. The role of the α -helix dipole in protein function and structure. *Prog Biophys Mol Biol.* 1985;45(3):149–95.
- Hornig JC, Demarest SJ, Raleigh DP. pH-dependent stability of the human alpha-lactalbumin molten globule state: contrasting roles of the 6–120 disulfide and the beta-subdomain at low and neutral pH. *Proteins.* 2003;52(2):193–202.
- Ikeguchi M, Kato S, Shimizu A, Sugai S. Molten globule state of equine beta-lactoglobulin. *Proteins.* 1997;27(4):567–75.
- Ikeguchi M, Sugai S. Contribution of disulfide bonds to stability of the folding intermediate of alpha-lactalbumin. *Int J Pept Protein Res.* 1989;33(4):289–97.
- Ikeguchi M, Sugai S, Fujino M, Sugawara T, Kuwajima K. Contribution of the 6-120 disulfide bond of alpha-lactalbumin to the stabilities of its native and molten globule states. *Biochemistry.* 1992;31(50):12695–700.
- Iwaoka M, Yosida D, Kimura N. Importance of the single amino acid potential in water for secondary and tertiary structures of proteins. *J Phys Chem B.* 2006;110(29):14475–82.
- Kendrew JC, Dickerson RE, Strandberg BE, Hart RG, Davies DR, Phillips DC, et al. Structure of myoglobin: a three-dimensional fourier synthesis at 2 Å resolution. *Nature.* 1960;185(4711):422–7.
- Kobayashi N, Harano Y, Tochio N, Nakatani E, Kigawa T, Yokoyama S, et al. An automated system designed for large scale NMR data deposition and annotation: application to over 600 assigned chemical shift data entries to the BioMagResBank from the Riken structural genomics/proteomics initiative internal database. *J Biomol NMR.* 2012;53(4):311–20.
- Kobayashi N, Iwahara J, Koshiba S, Tomizawa T, Tochio N, Güntert P, et al. KUIJIRA, a package of integrated modules for systematic and interactive analysis of NMR data directed to high-throughput NMR structure studies. *J Biomol NMR.* 2007;39(1):31–52.
- Lifson S, Roig A. On the theory of helix–coil transition in polypeptides. *J Chem Phys.* 1961;34(6):1963–74.
- Lin SH, Konishi Y, Denton ME, Scheraga HA. Influence of an extrinsic cross-link on the folding pathway of ribonuclease a. conformational and thermodynamic analysis of cross-linked (Lysine7-Lysine41)-ribonuclease a. *Biochemistry.* 1984;23(23):5504–12.
- Moriarty DF, Demarest SJ, Robblee J, Fairman R, Raleigh DP. Local interactions and the role of the 6-120 disulfide bond in alpha-lactalbumin: implications for formation of the molten globule state. *Biochim Biophys Acta.* 2000;1476(1):9–19.
- Nakagawa K, Tokushima A, Fujiwara K, Ikeguchi M. Proline scanning mutagenesis reveals non-native fold in the molten globule state of equine beta-lactoglobulin. *Biochemistry.* 2006;45(51):15468–73.
- Nakagawa K, Yamada Y, Fujiwara K, Ikeguchi M. Interactions responsible for secondary structure formation during folding of equine beta-lactoglobulin. *J Mol Biol.* 2007;367(4):1205–14.
- Pauling L, Corey RB, Branson HR. The structure of proteins; two hydrogen-bonded helical configurations of the polypeptide chain. *Proc Natl Acad Sci USA.* 1951;37(4):205–11.
- Peng ZY, Wu LC, Kim PS. Local structural preferences in the alpha-lactalbumin molten globule. *Biochemistry.* 1995;34(10):3248–52. <https://doi.org/10.1021/bi00010a014>
- Poland DC, Scheraga HA. Statistical mechanics of noncovalent bonds in polyamino acids. VIII. Covalent loops in proteins. *Biopolymers.* 1965;3(4):379–99. <https://doi.org/10.1002/bip.1965.360030404>
- Presta LG, Rose GD. Helix signals in proteins. *Science.* 1988;240(4859):1632–41.
- Ptitsyn OB. Molten globule and protein folding. *Adv Protein Chem.* 1995;47:83–229.
- Richardson JM, Makhataдзе GI. Temperature dependence of the thermodynamics of helix-coil transition. *J Mol Biol.* 2004;335(4):1029–37.
- Richardson JS, Richardson DC. Amino acid preferences for specific locations at the ends of α helices. *Science.* 1988;240(4859):1648–52.
- Sali A, Blundell TL. Comparative protein modelling by satisfaction of spatial restraints. *J Mol Biol.* 1993;234(3):779–815.
- Scheraga HA, Vila JA, Ripoll DR. Helix-coil transitions re-visited. *Bio-phys Chem.* 2002;101-102:255–65.

- Scholtz JM, Marqusee S, Baldwin RL, York EJ, Stewart JM, Santoro M, et al. Calorimetric determination of the enthalpy change for the alpha-helix to coil transition of an alanine peptide in water. *Proc Natl Acad Sci USA*. 1991;88(7):2854–8.
- Shoemaker KR, Kim PS, York EJ, Stewart JM, Baldwin RL. Tests of the helix dipole model for stabilization of α -helices. *Nature*. 1987;326(6113):563–7.
- Stapley BJ, Rohl CA, Doig AJ. Addition of side chain interactions to modified Lifson-Roig helix-coil theory: application to energetics of phenylalanine-methionine interactions. *Protein Sci*. 1995;4(11):2383–91.
- Wada A. The alpha-helix as an electric macro-dipole. *Adv Biophys*. 1976;9:1–63.
- Wedemeyer WJ, Scheraga HA. Exact analytical loop closure in proteins using polynomial equations. *J Comput Chem*. 1999;20(8):819–44.
- Wedemeyer WJ, Welker E, Narayan M, Scheraga HA. Disulfide bonds and protein folding. *Biochemistry*. 2000;39(23):7032.
- Wishart DS, Bigam CG, Holm A, Hodges RS, Sykes BD. ^1H , ^{13}C and ^{15}N random coil NMR chemical shifts of the common amino acids. I. Investigations of nearest-neighbor effects. *J Biomol NMR*. 1995;5(1):67–81.
- Wishart DS, Bigam CG, Yao J, Abildgaard F, Dyson HJ, Oldfield E, et al. ^1H , ^{13}C and ^{15}N chemical shift referencing in biomolecular NMR. *J Biomol NMR*. 1995;6(2):135–40.
- Yamada Y, Nakagawa K, Yajima T, Saito K, Tokushima A, Fujiwara K, et al. Structural and thermodynamic consequences of removal of a conserved disulfide bond from equine beta-lactoglobulin. *Proteins*. 2006;63(3):595–602.
- Yamada Y, Yajima T, Fujiwara K, Arai M, Ito K, Shimizu A, et al. Helical and expanded conformation of equine beta-lactoglobulin in the cold-denatured state. *J Mol Biol*. 2005;350(2):338–48.
- Yamamoto M, Nakagawa K, Fujiwara K, Shimizu A, Ikeguchi M. A native disulfide stabilizes non-native helical structures in partially folded states of equine beta-lactoglobulin. *Biochemistry*. 2011;50(49):10590–7.
- Yutani K, Ogasahara K, Kuwajima K. Absence of the thermal transition in apo-alpha-lactalbumin in the molten globule state. A study by differential scanning microcalorimetry. *J Mol Biol*. 1992;228(2):347–50.
- Zhang T, Bertelsen E, Alber T. Entropic effects of disulphide bonds on protein stability. *Nat Struct Biol*. 1994;1(7):434–8.
- Zimm BH, Bragg JK. Theory of the phase transition between helix and random coil in polypeptide chains. *J Chem Phys*. 1959;31(2):526–35.

SUPPORTING INFORMATION

Additional supporting information can be found online in the Supporting Information section at the end of this article.

How to cite this article: Yanagida Y, Yoshida K, Ohtomo M, Fujiwara K, Ikeguchi M. Mechanisms of helix induction by the closed loop. *Protein Science*. 2025;34(6):e70171. <https://doi.org/10.1002/pro.70171>